

# Multiobjective optimization of buffer capacity allocation in multiproduct unreliable production lines using improved adaptive NSGA-II algorithm

Jianguo Duan<sup>1,\*</sup>, Haochen Li<sup>2</sup>, Qinglei Zhang<sup>1</sup>

<sup>1</sup>China Institute of FTZ Supply Chain, Shanghai Maritime University, Shanghai, China

<sup>2</sup>Logistics Engineering college, Shanghai Maritime University, Shanghai, China

\*Corresponding Author: [jgduan@shmtu.edu.cn](mailto:jgduan@shmtu.edu.cn)

## Abstract

Buffer capacity allocation plays a key role in the design of production lines. By means of polymorphism analysis on production capacity and capability, we investigate the buffer allocation problem in multistage production lines with unreliable machines. The allocated buffers simultaneously maximize the system theoretical production rate and minimize the system state entropy. A mathematical model for buffer capacity optimization was established and optimized using an extended vector universal generating function (UGF) and an improved adaptive nondominated sorting genetic algorithm II (NSGA-II). The feasibility and effectiveness of the proposed method were verified by applying the model to a production line of engine heads.

**Keywords:** Buffer allocation; multi-state reliability; repairable production system; structural complexity.

## 1. Introduction

### 1.1 Research motivation

The normal operation of a production line is seriously affected by various uncertainties (Gershwin *et al.*, 2018). Some uncertainties can be compensated by systematic flexibility, whose extent is rather limited. In most cases, the relationships between production uncertainties and flexibility are balanced by arranging a certain number of buffers between workstations (Shi *et al.*, 2016). It has always been a key issue in production line design to create enough space in buffer stations for the storage of Work in Process and minimize the equipment cost and maintenance cost brought about by the intermediate buffers while avoiding time waste and logistics interruption due to excessive travel of Work in Process in intermediate buffers, and maintaining the reliability, controllability, and stability of operations (Sabuncuoglu *et al.*, 2006; Staley *et al.*, 2012; Gan *et al.*, 2013 and 2015). Among these aspects, system modeling and evaluation lay the basis for buffer capacity distribution, while reasonable allocation solutions are obtained by means of the optimization method (Ng *et al.*, 2017). Therefore, it is of great significance to study the allocation method and optimization algorithm of buffer capacity on account of analyzing multistate reliability and structural complexity for production line design.

### 1.2 Literature review

As an essential and complicated part of production line design, buffer capacity allocation has drawn much attention for more than fifty years. Enginarlar *et al.* (2002) investigated the smallest level of buffering to ensure the desired production rate in serial lines with unreliable machines. Konishi (2010) studied the blockage and starvation of a buffered production line from the viewpoint of nonlinear dynamics. Sana (2012) determined the optimum buffer level and production run time by trading off the holding cost, shortage cost, rework cost, repair cost for warranty, labor/energy costs, material cost, and maintenance cost. Kose *et al.* (2015) developed a hybrid simulation optimization approach based on evolutionary algorithm to optimize two conflicting objectives, which included the maximization of average system production rate and the minimization of total buffer size. Sabry *et al.* (2017) studied the performance of reliable, unpaced merging assembly lines with asymmetric buffer storage sizes. Radhoui *et al.* (2009) developed an integrated model considering preventive maintenance, quality control, and buffer sizing for unreliable and imperfect production systems. Walid *et al.* (2011) explored the effects of buffer size on attenuating the impact of line blockage

and starvation, examined the measures of performance, and addressed the throughput of an automated production line in processing multiple products. Matta *et al.* (2011) proposed a sequential search procedure based on a Kriging approximation of the output function to optimize production systems with unreliable machines and interoperational buffers with limited capacity. Papadopoulos *et al.* (2013) experimentally studied a total of 105 buffer allocation issues of serial production lines using five different search algorithms including simulated annealing, genetic, Tabu search, myopic, and complete enumeration to record the throughput achieved and CPU time required. Gershwin *et al.* (2000), Demir *et al.* (2014), and Weiss *et al.* (2018) took some comprehensive surveys on the state of the art on buffer allocation problems. In these articles, literatures on buffer allocation with respect to various versions of optimization approaches, applicable solution methods, and the consideration of realistic or common test instances were classified and reviewed.

Modeling is the first and crucial step. Some traditional techniques such as Bayesian network, Petri net, and binary decision diagram do not work for multistate manufacturing systems due to the great number of states. The recently emerged UGF technique has been proved to be effective for the reliability evaluation of multistate manufacturing system without buffer stations but was hardly used in the evaluation of system complexity nor in solving buffer allocation problems of multistate manufacturing system with finite buffer stations integrated with stochastic process and multi-objective optimization.

The proposed research in this paper overcomes the above limitations with respect to the following:

(1) In order to describe the diversity of production capability and the size of production capacity simultaneously in one function, we propose an improved vector UGF. Hence, the reliability of nonserial multistate repairable production line with finite buffers is measured through analysis of the effects of the buffers' states on the machines' states and decomposition of the system configuration. By replacing combinational operation with the algebraic operation, the problem of combination explosion during reliability modeling with stochastic process method is eliminated.

(2) The traditional complexity models are established on the assumption that all states are mutually independent, but in fact it is not true. We use the proposed vector UGF and state entropy to model the structural complexity of multistate manufacturing system with finite buffers. This

technique can evaluate the system structural complexity precisely from the system level meanwhile overcoming the shortcomings of the existing methods with the assumption of state independence and ensure the accurate and quantitative evaluation of system state uncertainties.

(3) Taking the system multistate reliability and system structural complexity as the optimization objective functions, buffer stations of the production line are optimally configured with the tools of the extended vector UGF and improved adaptive NSGA-II algorithm. This method can formulate the buffer allocation problems as a function of the system structure and the performance distributions of its elements and discover the optimal composition of all the factors influencing the entire system performance subject to specific constraints efficiently. The optimization solutions give some practical proposals for the design and planning of multiproduct unreliable production lines with multiple stages and nonserial configurations, such as engine-head machining lines.

### 1.3 Outline

The remainder of this paper is organized as follows: in Section 2, the multiproduct repairable production system is described, and 6 assumptions are proposed as the basis for follow-up work. In Section 3, full details of the proposed machine modeling approach are provided, including the actual steady-state probability under various states and non-steady-state probability. The vector UGF model of machines is also included in this section. Full calculation procedures for vector UGF of the entire system and their composition operators are defined in Section 4. In addition, two indicators including multistate reliability and structural complexity, accompanied with relevant measures, are also given in this section. Optimal allocation method of buffer capacity including problem formulation, optimization algorithm, and equality constraints is illustrated in Section 5, followed by a case study in Section 6 and conclusions in Section 7.

## 2. Problem statement and assumptions

It is assumed that there is a repairable serial-parallel multistate production line with  $m$  unreliable workstations and  $m-1$  intermediate buffers for part family  $\mathbf{P} = \{P_1, P_2, \dots, P_K\}$ . Each element of  $\mathbf{P}$  indicates one part. Each workstation  $i$  ( $i=1, \dots, m$ ) has  $n_i$  identical machines, where  $n_i$  is a strictly positive integer. All machines are identical, while the numbers may be different. Buffer stations are placed between every two workstations. Assume that the

$j$ th machine located in workstation  $i$  is denoted as  $M_{ij}$ , and it possesses  $m_{ij}$  performance levels, represented by vector  $\mathbf{g}_{ij} = \{g_{ij1}, \dots, g_{ijm_{ij}}\}$ .  $k$  is the state of a machine, and  $g_{ijk}$  is the performance level of machine  $M_{ij}$  in state  $k$ , where  $k=1, \dots, m_{ij}$ . Let  $g_{ij1}$  represent the worst (complete failure) and let  $g_{ijm_{ij}}$  represent the best performance condition. Performance rate  $G_{ij}(t)$  at any moment  $t \geq 0$  is a random variable, where  $G_{ij}(t) \in g_{ij}$ , and its corresponding state and probability are

$$X_{ij}(t) \in \mathbf{x}_{ij} = \{1, \dots, m_{ij}\}, \mathbf{p}_{ij} = \{p_{ij1}, p_{ij2}, \dots, p_{ijm_{ij}}\}$$

Consisting of state combinations of all machines, the number of system states is

$$K = \prod_{i=1}^m \left( \prod_{j=1}^{n_i} m_{ij} \right)$$

In order to evaluate the performance distribution of the entire system, all possible performances and their corresponding state probabilities are required. Aiming to describe more clearly the multistate reliability modeling issue of repairable production lines with finite buffers, the study is based on the following assumptions:

(1) Each machine  $j, j=1, \dots, n_i$ , of workstation  $i, i=1, \dots, m$ , in the line is to be repaired in time if it fails, and the highest performance level (state  $m_{ij}$ ) is completely restored after repair. Machining time, failure time, and repair time of  $M_{ij}$  follow exponential distributions, respectively.

(2) For all part types in the part family, the buffer capacity remains constant, and there is no failure during workpiece transition.

(3) Compared to production rates, the time of workpieces stored in or removed from buffer stations is short and negligible.

(4) All machines located in workstation 1 are never starved, and all machines located in the last workstation are never blocked.

(5) When buffer station  $i$  is full, all machines in workstation  $i-1$  are shut down after processing an additional workpiece, and all machines in workstation  $i+1$  will keep working if there is no failure.

(6) When buffer station  $i$  has no spare workpiece, machines located in workstation  $i+1$  are idle due to material shortage and will be shut down for standby.

### 3. Machine modeling

#### 3.1 State probability calculation

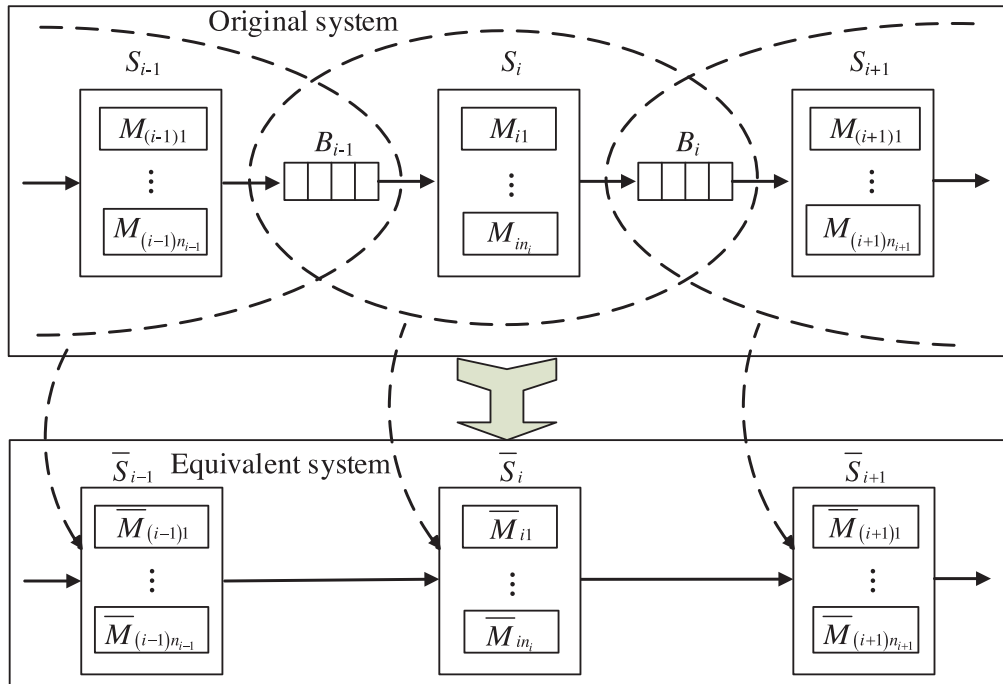


Fig. 1. Production system with buffer stations.

Figure 1 shows a part of the production line.  $S_i$  denotes workstation  $i$  and  $B_i$  represents buffer station  $i$ . Suppose that the capacity of  $B_i$  is  $b_i$ , the production rate of  $S_i$  is  $\omega_i$ , and that of  $S_{i+1}$  is  $\omega_{i+1}$ . According to literature (Shu *et al.*, 1992), the steady-state solution is obtained by establishing the state transition equation of  $B_i$ . The probability of  $c$  ( $c=0,1,\dots,b_i$ ) workpieces staying in  $B_i$  is obtained by

$$P_{ic}^B = \frac{\rho_i^c (1 - \rho_i)}{1 - \rho_i^{b_i+1}} \quad (1)$$

where  $\rho_i = \omega_i / \omega_{i+1}$ . When  $\omega_i = \omega_{i+1}$ ,  $\rho_i = 1$  and  $P_{ic}^B = 1 / (b_i + 1)$ .

Thus, the probability that  $B_i$  is not empty can be obtained by

$$P_{i0}^B = 1 - P_{i0}^B = \frac{\rho_i (1 - \rho_i^{b_i})}{1 - \rho_i^{b_i+1}} \quad (2)$$

The probability that  $B_i$  is not full can be obtained by

$$P_{ib_i}^B = 1 - P_{ib_i}^B = \frac{1 - \rho_i^{b_i}}{1 - \rho_i^{b_i+1}} \quad (3)$$

When  $B_i$  is full, all the machines of workstation  $S_i$  will be stopped due to overloading. When  $B_i$  is empty, all the machines in workstation  $S_{i+1}$  will be stopped due to material shortage. All the machines of workstation  $S_i$  work normally only when  $B_{i-1}$  has spare workpieces and  $B_i$  has spare space. Thus, the actual steady-state probability of machine  $M_{ij}$  in state  $k$  is obtained by

$$\tilde{P}_{ijk} = \frac{P_{(i-1)0}^B P_{ijk} P_{ib_i}^B}{(1 - \rho_{i-1}^{b_{i-1}+1})(1 - \rho_i^{b_i+1})} P_{ijk} \quad (4)$$

The probability of machine  $M_{ij}$  failing to remain in state  $k$  due to blockage, material shortage, or machine failures is obtained by

$$\bar{P}_{ijk} = \left( 1 - \frac{\rho_{i-1} (1 - \rho_{i-1}^{b_{i-1}})(1 - \rho_i^{b_i})}{(1 - \rho_{i-1}^{b_{i-1}+1})(1 - \rho_i^{b_i+1})} \right) P_{ijk} \quad (5)$$

Assume that all machines in the first workstation possess enough workpieces, and then the actual steady-state and non-steady-state probabilities of machine  $M_{1j}$  in state  $k$  ( $2 \leq k \leq m_{1j}$ ) are obtained, respectively, by

$$\begin{aligned} \tilde{P}_{1jk} &= \frac{1 - \rho_1^{b_1}}{1 - \rho_1^{b_1+1}} P_{1jk} \\ \bar{P}_{1jk} &= \frac{\rho_1^{b_1} (1 - \rho_1)}{1 - \rho_1^{b_1+1}} P_{1jk} \end{aligned} \quad (6)$$

Assuming that all the machines in the last workstation possess enough stock space to ensure smooth output, the actual steady-state probability and non-steady-state probability of machine  $M_{mj}$  of workstation  $S_m$  in state  $k$  ( $2 \leq k \leq m_{ij}$ ) are obtained, respectively, by

$$\begin{aligned} \tilde{P}_{mjk} &= \frac{\rho_{m-1} (1 - \rho_{m-1}^{b_{m-1}})}{1 - \rho_{m-1}^{b_{m-1}+1}} P_{mjk} \\ \bar{P}_{mjk} &= \frac{1 - \rho_{m-1}}{1 - \rho_{m-1}^{b_{m-1}+1}} P_{mjk} \end{aligned} \quad (7)$$

Based on the above analyses,  $M_{ij}$  is equated to  $\bar{M}_{ij}$  through Equations (4)-(7). Consequently, the original production system is transferred to an equivalent system as shown in Figure 1.

### 3.2 Machine UGF calculation

The performance of production line is affected by the characteristics of machines as well as the arrangement of them within the system. Hence, it may have a finite number of performance levels and belongs to the category of multistate manufacturing systems. At any specific time, the machine in the system is in a specific state. The combination of these states determines the working state of the system at that time; that is, the state of the system is determined by the state of each machine in the system.

Traditionally, Boolean-based methods (Dinkar *et al.*, 2018) (such as minimal cut sets and the fault-tree technique) and stochastic-based methods (Khan *et al.*, 2018; Verma *et al.*, 2013) (such as mainly Markov and semi-Markov processes) are used to evaluate the performance of multistate systems. But, for the large multistate systems, these techniques are especially incompetent and extremely time consuming because of the high number of system states. The UGF technique has been proved to be efficient in evaluating the availability and reliability of large multistate systems (Youssef, *et al.*, 2008). It employs algebra operations to determine the performance distribution of multistate systems, instead of combination operation, and avoid the combination explosion of multistate systems. In recent years, it has become a new tool to analyze the system performance.

The state space of the entire system increases exponentially with the growing of machines and buffer stations, which makes it extremely difficult and even impossible to proceed for a large system. However, UGF technique is an appropriate and efficient tool for such condition. The  $u$ -function  $u_{ij}(z)$  representing the performance rate of machine  $M_{ij}$  in consideration of the

buffer states' influence is given by

$$u_{ij}(z) = \sum_{k=1}^{m_{ij}} \tilde{p}_{ijk} z^{g_{ijk}} \quad (8)$$

where  $\tilde{p}_{ijk}$  is the actual steady-state probability when the performance vector is  $g_{ijk}$ .

Machines exhibit corresponding steady-state probabilities during the process of machining various workpieces, which is expressed with vectors; thus, the earlier  $u$ -function evolves to

$$u_{ij}(z) = \sum_{k=1}^{m_{ij}} \tilde{p}_{ijk} z^{g_{ijk}} \quad (9)$$

## 4. System modeling

### 4.1 System UGF calculation

The probability and performance rate in each state are expressed with vectors that possess the same dimensions as the workpiece types  $K$ . Consequently, the equivalent production systems are divided into independent parallel subsystems and serial subsystems. The system  $u$ -function  $\tilde{U}_s(z)$  is derived through recursive decomposition, and the final results are evaluated by the equivalent modules and operators, both parallel and serial.

$$\begin{aligned} \tilde{U}_s(z) &= \otimes(\tilde{U}_1(z), \tilde{U}_2(z)) \\ &= \otimes\left(\sum_{i=1}^{c_1} \tilde{p}_{1i} z^{g_{1i}}, \sum_{j=1}^{c_2} \tilde{p}_{2j} z^{g_{2j}}\right) \\ &= \sum_{i=1}^{c_1} \sum_{j=1}^{c_2} \tilde{p}_{1i} \tilde{p}_{2j} z^{\phi(g_{1i}, g_{2j})} \end{aligned} \quad (10)$$

where  $\tilde{U}_1(z)$ ,  $\tilde{U}_2(z)$  are  $u$ -functions of equivalent subsystems 1, 2;  $c_1$ ,  $c_2$  are state numbers of subsystems 1, 2;  $\tilde{p}_{1i}$ ,  $\tilde{p}_{2j}$  are probability vectors corresponding to performance vectors  $g_{1i}$ ,  $g_{2j}$

$$\tilde{p}_{1i} = [\tilde{p}_{1i}^1 \quad \tilde{p}_{1i}^2 \quad \cdots \quad \tilde{p}_{1i}^K]^T, \tilde{p}_{2j} = [\tilde{p}_{2j}^1 \quad \tilde{p}_{2j}^2 \quad \cdots \quad \tilde{p}_{2j}^K]^T$$

$\tilde{U}_s(z)$  is  $u$ -functions of the entire system  $S$  which is

composed by equivalent subsystems 1 and 2.

Serial and parallel composition operators in vector are defined as follows:

(1) Serial composition operator:

$$\begin{aligned} \sigma(\tilde{U}_1(z), \tilde{U}_2(z)) &= \sigma\left(\sum_{i=1}^{c_1} \tilde{p}_{1i} z^{g_{1i}}, \sum_{j=1}^{c_2} \tilde{p}_{2j} z^{g_{2j}}\right) = \sum_{i=1}^{c_1} \sum_{j=1}^{c_2} \tilde{p}_{1i} \tilde{p}_{2j} z^{\min(g_{1i}, g_{2j})} \\ &= \sum_{i=1}^{c_1} \sum_{j=1}^{c_2} \begin{bmatrix} \tilde{p}_{1i}^1 \\ \tilde{p}_{1i}^2 \\ \vdots \\ \tilde{p}_{1i}^K \end{bmatrix} \begin{bmatrix} \tilde{p}_{2j}^1 \\ \tilde{p}_{2j}^2 \\ \vdots \\ \tilde{p}_{2j}^K \end{bmatrix} z^{\begin{bmatrix} \min(g_{1i}^1, g_{2j}^1) \\ \min(g_{1i}^2, g_{2j}^2) \\ \vdots \\ \min(g_{1i}^K, g_{2j}^K) \end{bmatrix}} = \sum_{i=1}^{c_1} \sum_{j=1}^{c_2} \begin{bmatrix} \tilde{p}_{1i}^1 \tilde{p}_{2j}^1 \\ \tilde{p}_{1i}^2 \tilde{p}_{2j}^2 \\ \vdots \\ \tilde{p}_{1i}^K \tilde{p}_{2j}^K \end{bmatrix} z^{\begin{bmatrix} \min(g_{1i}^1, g_{2j}^1) \\ \min(g_{1i}^2, g_{2j}^2) \\ \vdots \\ \min(g_{1i}^K, g_{2j}^K) \end{bmatrix}} \end{aligned}$$

(2) Parallel composition operator:

$$\begin{aligned} \pi(\tilde{U}_1(z), \tilde{U}_2(z)) &= \pi\left(\sum_{i=1}^{c_1} \tilde{p}_{1i} z^{g_{1i}}, \sum_{j=1}^{c_2} \tilde{p}_{2j} z^{g_{2j}}\right) = \sum_{i=1}^{c_1} \sum_{j=1}^{c_2} \tilde{p}_{1i} \tilde{p}_{2j} z^{g_{1i} + g_{2j}} \\ &= \sum_{i=1}^{c_1} \sum_{j=1}^{c_2} \begin{bmatrix} \tilde{p}_{1i}^1 \\ \tilde{p}_{1i}^2 \\ \vdots \\ \tilde{p}_{1i}^K \end{bmatrix} \begin{bmatrix} \tilde{p}_{2j}^1 \\ \tilde{p}_{2j}^2 \\ \vdots \\ \tilde{p}_{2j}^K \end{bmatrix} z^{\begin{bmatrix} g_{1i}^1 + g_{2j}^1 \\ g_{1i}^2 + g_{2j}^2 \\ \vdots \\ g_{1i}^K + g_{2j}^K \end{bmatrix}} = \sum_{i=1}^{c_1} \sum_{j=1}^{c_2} \begin{bmatrix} \tilde{p}_{1i}^1 \tilde{p}_{2j}^1 \\ \tilde{p}_{1i}^2 \tilde{p}_{2j}^2 \\ \vdots \\ \tilde{p}_{1i}^K \tilde{p}_{2j}^K \end{bmatrix} z^{\begin{bmatrix} g_{1i}^1 + g_{2j}^1 \\ g_{1i}^2 + g_{2j}^2 \\ \vdots \\ g_{1i}^K + g_{2j}^K \end{bmatrix}} \end{aligned}$$

For the serial-parallel production system, the process of calculating system  $u$ -function is as follows:

(1) Decompose the structure of the equivalent system in consideration of buffer states.

(2) Calculate the UGFs of all parallel equivalent subsystems using Equation (9) and parallel composition operator.

(3) Simplify the serial-parallel hybrid production system into a serial system.

(4) Calculate  $\tilde{U}_s(z)$  of the entire equivalent system using serial composition operator as shown in Figure 2.

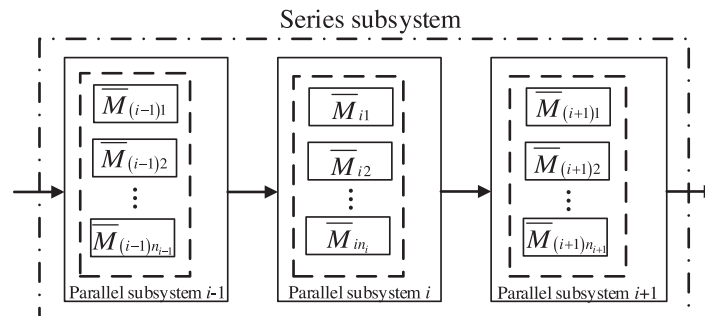


Fig. 2. Decomposition of systems.



## 4.2 Performance indicators

Let the system have a total of  $M$  states, and let the state vector space be

$$\mathbf{g}_s = \{\mathbf{g}_1^s, \mathbf{g}_2^s, \dots, \mathbf{g}_M^s\}$$

where the corresponding probability vector space is

$$\mathbf{p}_s = \{\mathbf{p}_1^s, \mathbf{p}_2^s, \dots, \mathbf{p}_M^s\}$$

The  $i$ -th state vector and probability vector, respectively, are

$$\mathbf{g}_i^s = [g_{i1}^s \ g_{i2}^s \ \dots \ g_{iK}^s]^T, \quad \mathbf{p}_i^s = [p_{i1}^s \ p_{i2}^s \ \dots \ p_{iK}^s]^T$$

We describe the behavior of a multistate production line in terms of reliability via the improvement of a parameter that is defined by ameliorating the classical reliability indicator. Reliability is defined as a measure of how much a system can fulfill the requirements of a certain performance level. System multistate reliability, thus, can be evaluated by systematic theoretical production rate  $E_s(z)$  by operator  $\delta_E$ .

$$E_s(z) = \delta_E(\tilde{U}_s(z)) = \delta_E\left(\sum_{i=1}^M \mathbf{p}_i^s z^{\mathbf{g}_i^s}\right) = \sum_{i=1}^M \mathbf{p}_i^s \mathbf{g}_i^s \quad (11)$$

State identification and calculation are fundamental for studying the structural complexity of a production system, depending on the research purpose and granularity of the production system. Actually, more attention is paid to the overall performance of the production system. From the standpoint of operability, events related to production capacity of the production system are taken as states utilized for complexity calculation, such as full-operation state, failure state, and a variety of discrete degraded states between them.

Entropy is a measure of information content. Its eigenvalues represent the uncertainties of the existing and operating states of the system. Entropy is widely used to measure uncertainties in deterministic phenomena. The greater the information entropy, the higher the systematic uncertainties. According to the definition of information entropy, the state entropy of the production line can be defined as

$$H_s = -\sum_{i=1}^M \sum_{j=1}^K p_{ij}^s \log_2 p_{ij}^s \quad (12)$$

where  $p_{ij}^s$  is the probability corresponding to the state  $g_{ij}^s$ ,  $1 \leq i \leq M$ .

## 5. Buffer allocation

### 5.1 Optimal allocation model

With the aim of designing and planning more productive and predictive manufacturing systems, nonlinear behavior of production systems needs to be comprehended and controlled. Consequently, a mathematical model for optimized allocation of buffer capacity based on reliability and complexity of the production system is established in this paper.

$$E_{\max}(b_1, \dots, b_{m-1}) = \max \sum_{j=1}^K E_j^s \quad (13)$$

$$H_{\min}(b_1, \dots, b_{m-1}) = \min H_s \quad (14)$$

$$\text{s.t.} \quad \sum_{i=1}^{m-1} b_i \leq B \quad (15)$$

$$b_i \geq b_{\min} \quad (16)$$

$$E_j^s \geq e_{\min} \quad j = 1, 2, \dots, m-1 \quad (17)$$

$$b_i, B, b_{\min} \in \mathbb{Z}^+ \quad E_j^s, e_{\min} \in \mathbb{R}^+$$

where  $E_j^s$  is the  $j$ -th component of systematic theoretical production rate, that is, the systemic theoretical productivity achieved while machining part  $P_j$ .  $\sum E_j^s$  represents the sum of theoretical production rates achieved while machining part family  $\mathbf{P} = \{P_1, P_2, \dots, P_K\}$ .  $b_i$  represents the capacity of the  $i$ -th buffer station.  $B$  denotes the maximum total buffer capacity allowable by system.  $b_{\min}$  denotes the minimum buffer capacity allocated to each buffer station and  $b_{\min} = 4$  in discrete systems.  $e_{\min}$  is the minimum theoretical productivity achieved while machining each part. Constraint (15) is the upper bound of total buffer capacity. Constraint (16) is the lower bound of each buffer capacity. Constraint (17) denotes that the machining capability for each part is no less than the minimum allowable theoretical productivity.

### 5.2 Optimal allocation algorithm

Buffer capacity allocation is a combinatorial optimization issue. According to the mathematical model established in this paper, there are mainly two kinds of problems: ① multiple constraints and conflicting objectives; ② high dimensional search space with complex parameter restrictions. The traditional algorithms, such as weighting method (Sabir *et al.*, 2018), constraints, and linear programming, cannot reach collaborative optimization of all indicators and converge to the nonconvex surface of Pareto optimal front for the two fitness functions.

Therefore, a good multi-objective optimization algorithm is the key to solve the problem.

Deb et al. proposed NSGA-II algorithm with elite strategy in 2002. Compared with NSGA, this algorithm has better convergence speed, much lower computational complexity (from  $O(MN^3)$  to  $O(MN^2)$ ), and smaller solution error caused by artificially specified parameters. Its good performance was widely used in solving multi-objective problems. However, NSGA-II is also easy

to make the remaining nondominated solutions pile up at the front of Pareto, resulting in the phenomenon of zero crowding degree and loss of population diversity. Therefore, in view of the objectives concerned in this paper and the shortcomings of NSGA-II algorithm, an improved NSGA-II algorithm with adaptive strategy is used to solve the optimal allocation model, and a set of Pareto optimal fronts that meet the actual requirements are obtained. Figure 3 illustrates the flowchart of the proposed algorithm.

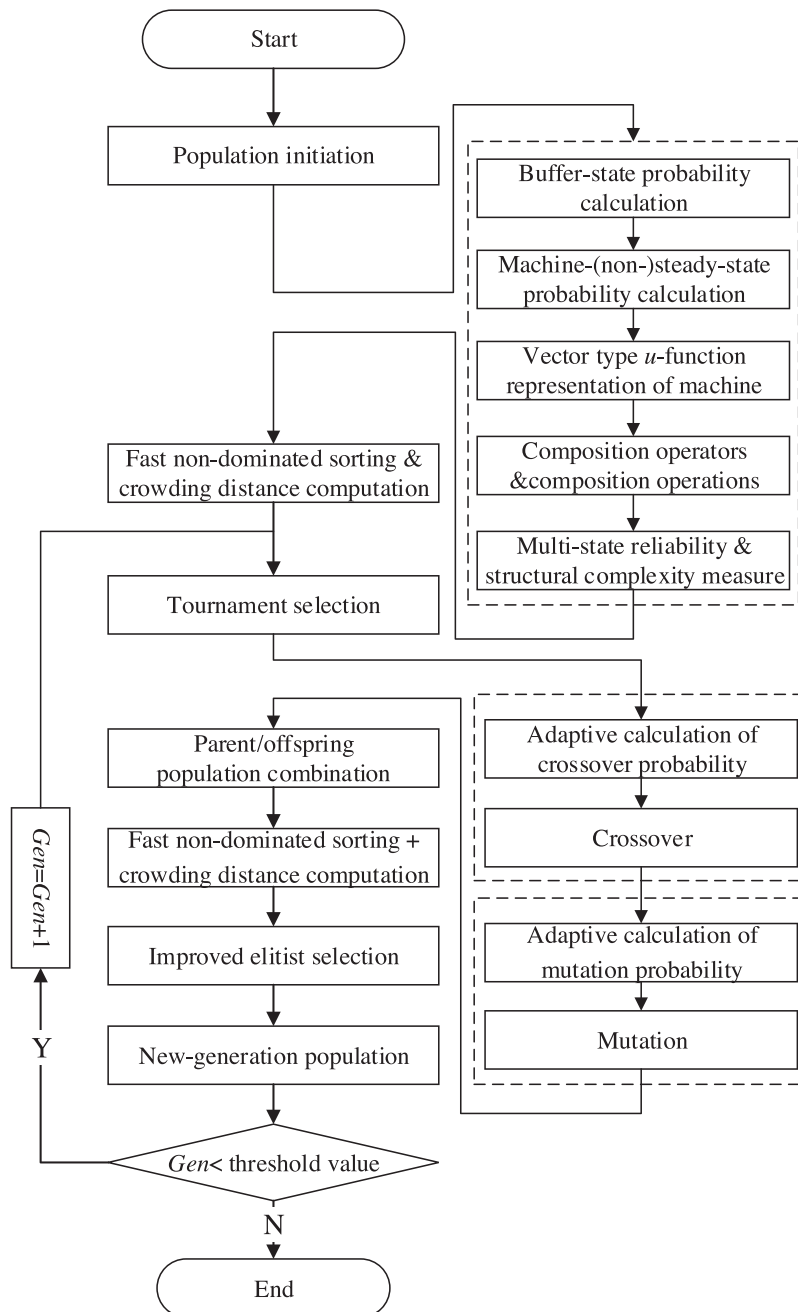


Fig. 3. Flowchart of the proposed algorithm.

(1) Population initialization: in order to ensure the diversity of population, and to traverse the solution space as much as possible, this paper constructs the initial population by randomly generating chromosomes according to constraints (15)–(17). Coding is the key to solve the problem. Good coding is the bridge between the problem space and the search space of the optimization algorithm, and it is the core and primary goal of the algorithm to realize the optimization function. Integer is utilized to represent the parameter space. Suppose that there are nine buffer stations in a production line to which the capacity is allocated, and the order that the parts flow through the buffer is  $b_1 \rightarrow b_9$ , then the encoded buffer stations are represented as the chromosome shown in Figure 4.

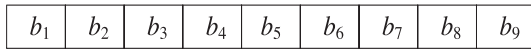


Fig. 4. Diagram of chromosome structure.

(2) Fast nondominated sorting and calculation of individual crowding degree: after generating the initial population, the nondominated sorting of individuals is operated. The fitness function is  $F(x) = \{E_{\min}(b_1, \dots, b_{m-1}), H_{\min}(b_1, \dots, b_{m-1})\}$ . The standard criterion is that if and only if the fitness value of  $x_1$  is not more than that of  $x_2$ , individual  $x_1$  dominates individual  $x_2$ , recorded as  $x_1 < x_2$ . After generating the first layer of Pareto, the individuals in Pareto are excluded from the population, and the remaining individuals continue to be ranked according to the level of noninferior solution until all the individuals have their corresponding sequence number. At the same time, the crowding distance of individuals in the same layer is calculated. The individual with the largest fitness value in each layer is regarded as the boundary, and its crowding degree is set as infinite. Other individuals' crowding degree is the sum of differences between the fitness values of the two neighboring individuals.

(3) Self-adaptive crossover and mutation operations. To avoid the limitation of confirming crossover probability and mutation probability, we propose an adaptive strategy for crossover and mutation operations, which can not only ensure the global and local search ability of the algorithm, but also dynamically adjust the evolution direction of the population during iteration, so as to improve the adaptability of the algorithm in the solution space.

Adaptive strategy: crossover probability and mutation probability change with the evolution of population. In the early stage, individuals are more dispersed in solution

space. So, crossover and mutation probabilities with smaller value can improve the convergence speed and determine the direction of convergence. In the later stage, in order to prevent the solution space from falling into the local optimal solution, they can be appropriately increased to maintain population diversity.

Denote the total evolutionary generation as  $Gen$ , and the adaptive crossover probability  $P_c(i)$  and mutation probability  $P_m(i)$  can be calculated by

$$P_c(i) = \min P_c + (\max P_c - \min P_c) \times \frac{i}{Gen} \quad (18)$$

$$P_m(i) = \min P_m + (\max P_m - \min P_m) \times \frac{i}{Gen} \quad (19)$$

In this research, two-point crossover is used, as shown in Figure 5. Randomly select two points in parent  $P_1$ , and determine the corresponding number and its position in parent  $P_2$ . To ensure that the generated offspring are also feasible solutions, select different buffer stations on  $P_1$  and  $P_2$  for crossover.

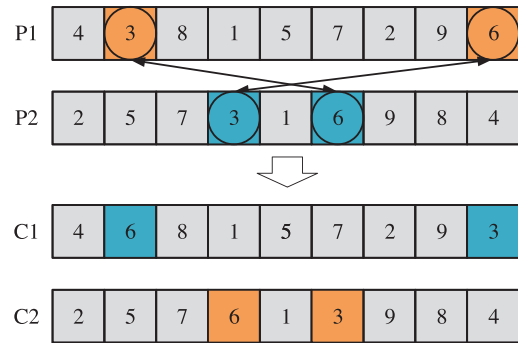


Fig. 5. The example of mutation operation.

In this paper, two-point exchange mutation is used, as shown in Figure 6. Randomly select two points in parent and exchange them to generate a new chromosome.

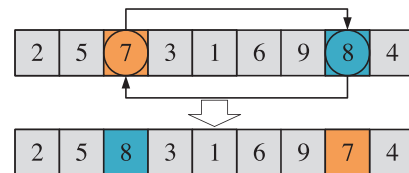


Fig. 6. The example of crossover operation.

(4) Improved elitist selection strategy. In this paper, an improved strategy of elite individual selection is proposed, which aims to improve the population diversity of offspring by introducing a distribution function (defined as Equation (20)) to limit excellent individuals in the nondominant front to the next generation of parents.



$$n_i = F_i \times r_i \quad (20)$$

where  $n_i$  is the number of chromosomes selected to the next generation,  $F_i$  is the total number of chromosomes in the  $i$ -th nondominated front, and  $r_i$  is a random number from 0.8 to 1.

### 6. Case study

In this section, a practical case of a production line located in south China for machining 2 distinct engine heads is reviewed as shown in Figure 7.

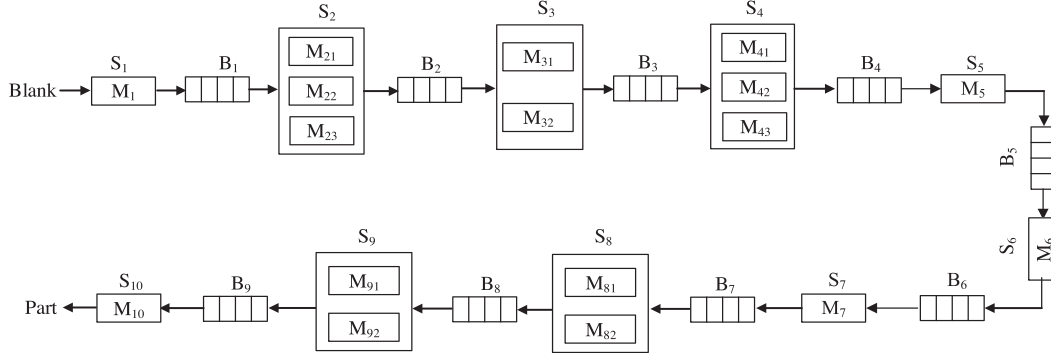


Fig.7. Engine head production line with 10 workstations and 9 intermediate buffers.

This production line consists of 10 workstations ( $S_1$ - $S_{10}$ ) and 9 intermediate buffer stations ( $B_1$ - $B_9$ ). Workstation  $S_1$  possesses only one machine  $M_1$ . Each of  $S_3$ ,  $S_8$  and  $S_9$  consists of 2 identical paralleled machines ( $M_{31}$ ,  $M_{32}$ ), ( $M_{81}$ ,  $M_{82}$ ), and ( $M_{91}$ ,  $M_{92}$ ), and  $S_2$ ,  $S_4$  include 3 identical machines ( $M_{21}$ ,  $M_{22}$ ,  $M_{23}$ ), ( $M_{41}$ ,  $M_{42}$ ,  $M_{43}$ ), respectively.

$b_1$ - $b_9$  represent the capacity of the 9 buffer stations.  $S_5$ ,  $S_6$ ,  $S_7$  and  $S_{10}$  are auxiliary workstations, and  $M_5$ ,  $M_{10}$  are cleaning machines.  $M_6$  is a press-fit machine, and  $M_7$  is a leak detector.

The parameters of each machine are given in Table 1.

Table 1. Machine parameters.

Workstation	Machine	Productivity $\omega/(\text{pcs}\cdot\text{h}^{-1})$		$p_{ij}$	Workstation	Machine	Productivity $\omega/(\text{pcs}\cdot\text{h}^{-1})$		$p_{ij}$
		$P_1$	$P_2$				$P_1$	$P_2$	
$S_1$	$M_1$	18	20	0.940 5	$S_6$	$M_6$	50	50	0.840 4
$S_2$	$M_2$	7	8	0.922 8	$S_7$	$M_7$	60	60	0.842 9
$S_3$	$M_3$	10	11	0.937 6	$S_8$	$M_8$	11	13	0.948 1
$S_4$	$M_4$	7	7	0.915 2	$S_9$	$M_9$	14	15	0.947 7
$S_5$	$M_5$	35	35	0.861 5	$S_{10}$	$M_{10}$	35	35	0.861 5

We set population size  $N=200$ , generation number  $Gen=100$ ,  $\min P_c=0.4$ ,  $\max P_c=0.8$ ,  $\min P_m=0.1$ ,  $\max P_m=0.2$ ,  $b_{\min}=4$ ,  $e_{\min}=6$ . Figure 8 shows the distribution of 100 nondominated solutions with the proposed algorithm. Table 2 shows the first 10 solutions among them. Based on the experimental results, we see that there is indeed trade-off between the two concerned objectives.

Weighted summation of objectives approach was applied to verify the results of the proposed approach. The weights of two objectives—*sum of theoretical production rates* and *state entropy of the production line*—are defined as 0.5. Figure 9 shows the convergence curve of the

weighted genetic algorithm. The best value is -5.8042, in which the sum of theoretical production rates  $E$  is 16.7787 and state entropy of the production line  $H=5.1703$ , and its corresponding optimal allocation solution is  $b_1(23)$ ,  $b_2(21)$ ,  $b_3(23)$ ,  $b_4(10)$ ,  $b_5(28)$ ,  $b_6(29)$ ,  $b_7(29)$ ,  $b_8(15)$ ,  $b_9(22)$ . However, with the application of weighted summation approach, the range of the values is from -5.6531 to -5.5429. Although it has a slight difference with the best value -5.8042 obtained by weighted genetic algorithm, the proposed optimization algorithm can offer much more feasible solutions. Especially when taking some other factors such as cost and time into consideration, it is more effective and competitive.

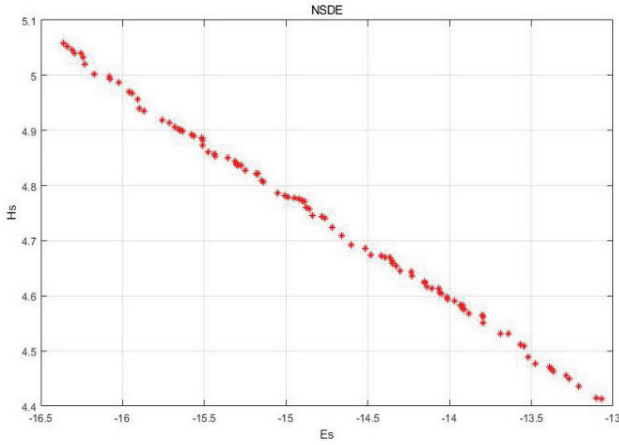


Fig. 8. Distribution of the found nondominated solutions.

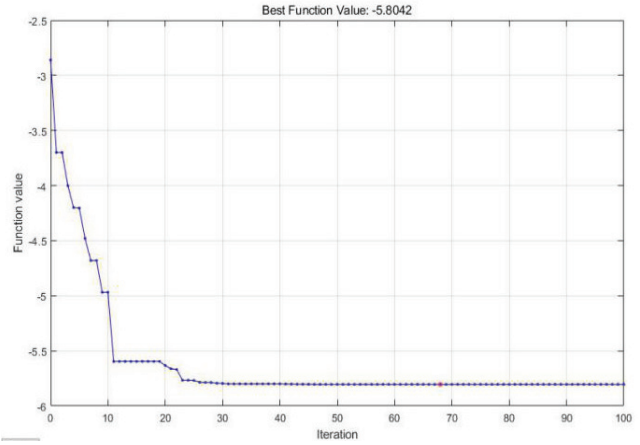


Fig. 9. Convergence curve of the weighted genetic algorithm.

Table 2. The top 10 nondominated solutions when  $B=200$ .

No.	Buffer capacity allocation									Total size $B$	Production rate $E_{\min}$	Structural complexity $H_{\min}$
	$B_1$	$B_2$	$B_3$	$B_4$	$B_5$	$B_6$	$B_7$	$B_8$	$B_9$			
1	22	30	28	10	25	19	30	15	21	200	16.3636	5.0575
2	23	30	28	10	23	20	29	15	21	199	16.3377	5.0517
3	25	29	28	10	23	19	29	15	21	199	16.3069	5.0455
4	24	30	27	11	23	19	29	15	21	199	16.2923	5.0401
5	23	30	28	10	23	19	29	15	21	198	16.2561	5.0397
6	22	30	28	11	23	19	29	15	21	198	16.2404	5.0322
7	23	30	28	10	23	19	26	20	21	200	16.2333	5.0197
8	25	30	28	13	23	19	29	16	17	200	16.1740	5.0014
9	23	25	39	10	23	19	24	15	21	199	16.0832	4.9969
10	26	30	33	10	23	19	22	15	21	199	16.0790	4.9932

In addition, two other experimental studies  $B=250$  and  $B=300$  are investigated to verify the influence of the total buffer size. Figure 10 depicts the distributions of the found nondominated solutions. According to this figure, in general, there are more nondominated solutions with the number increase of the total buffer size. When  $B=250$ , there are 112 feasible solutions, while when  $B=300$ , the number is 148. Table 3 and Table 4 list the top 10 nondominated solutions under the two situations.

Moreover, the peak values of both objectives become larger and larger with the increase of the total buffer size.

Analysis of all the test cases reveals that the variable total buffer size  $B$  to be allocated in the production line has a great impact on the system's reliability and controllability. The increasing capacity is helpful for us to improve the system's yields by smoothing the bottleneck workstations.



Fig. 10. Distributions of the found nondominated solutions when  $B=250$  and  $300$ , respectively.

Table 3. The top 10 nondominated solutions when  $B=250$ .

No.	Buffer capacity allocation									Total size $B$	Production rate $E_S$	Structural complexity $H_S$
	$B_1$	$B_2$	$B_3$	$B_4$	$B_5$	$B_6$	$B_7$	$B_8$	$B_9$			
1	18	36	34	14	35	20	40	21	32	250	17.5598	5.1552
2	17	36	34	14	35	20	40	21	32	249	17.4851	5.1498
3	16	36	34	14	35	20	40	21	32	248	17.4004	5.1436
4	18	36	34	14	35	18	40	21	32	248	17.3754	5.1318
5	18	38	34	14	35	20	32	21	32	244	17.3620	5.1287
6	18	36	34	16	35	17	40	21	32	249	17.2779	5.1159
7	19	35	38	13	27	21	32	27	32	244	17.2767	5.1019
8	17	40	34	20	23	24	34	22	32	246	17.1719	5.0973
9	18	41	35	12	25	20	34	28	32	245	17.1053	5.0859
10	17	44	37	17	23	24	28	26	32	248	17.0422	5.0654

Table 4. The top 10 nondominated solutions when  $B=300$ .

No.	Buffer capacity allocation									Total size $B$	Production rate $E_S$	Structural complexity $H_S$
	$B_1$	$B_2$	$B_3$	$B_4$	$B_5$	$B_6$	$B_7$	$B_8$	$B_9$			
1	26	24	35	24	45	29	36	28	29	276	18.4064	5.2471
2	29	37	45	21	39	23	30	24	47	295	18.3692	5.1901
3	27	34	59	21	34	27	28	24	39	293	18.3001	5.1743
4	25	37	49	21	39	23	30	24	32	280	18.1261	5.1619
5	25	36	49	21	39	23	28	24	32	277	18.0305	5.1533
6	21	34	59	22	34	25	28	24	39	286	17.9685	5.1480
7	22	37	49	21	39	23	28	24	32	275	17.9230	5.1454
8	24	36	49	21	26	28	29	22	33	268	17.8617	5.1376
9	25	36	56	23	43	18	33	23	29	286	17.8602	5.1237
10	25	35	49	21	27	23	32	24	32	268	17.7835	5.1235

## 7. Conclusions

In this paper, the buffer state functions are constructed, the influence of buffer capacity on the steady-state availability of production equipment is analysed, and the  $u$ -function of the entire system is calculated by means of extended vector UGF. Two indicators including multistate reliability and structural complexity, as well as their corresponding measures, are developed, respectively. From the above, the mathematical model of buffer capacity distribution is established, and a GA-based optimization algorithm is developed. By means of this method, not only are the “state dimension explosion” and equipment state coupling problem effectively overcome, but the complexity of realizing the accurate description of the system state is also greatly reduced. It is very suitable for reliability and complexity analysis in large-scale multistate production systems, as well as the systematic performance and structural synthesis and optimization.

In addition, an adaptive multi-objective optimization approach is proposed to solve the buffer allocation problem of multistate manufacturing systems. Although the complexity is remarkably reduced, a certain randomness is generated due to unreasonable parameter selection. Therefore, it is a key issue to figure out the way of improving the rationality in selection of evaluating indicators and developing a multi-objective optimization algorithm with better objectivity and reasonability to further improve the rationality of buffer allocation.

## ACKNOWLEDGEMENTS

This research is partially supported by the National Natural Science Foundation of China (51875332), the Capacity Building Projects of Some Local Universities of Shanghai Science and Technology Commission (18040501600).

## References

**Demir, L., Tunali, S. & Eliiyi, D.T. (2014).** The state of the art on buffer allocation problem: a comprehensive survey. *Journal of Intelligent Manufacturing*, **25**: 371-392.

**Dinkar, B.K. & Alok, K.M. (2018).** Reliability investigation of diesel engines used in dumpers by the Bayesian approach. *Kuwait Journal of Science*, **45**(4): 15-25.

**Enginarlar, E., Li, J.S., Meerkov, S.M. & Zhang, R.Q. (2002).** Buffer capacity for accommodating machine downtime in serial production lines. *International Journal*

*of Production Research*, **40**(3): 601-624.

**Gan, S.Y., Zhang, Z.H., Zhou, Y.F. & Shi, J.F. (2013).** Intermediate buffer analysis for a production system. *Applied Mathematical Modelling*, **37**: 8785-8795.

**Gan S.Y., Zhang, Z.S., Zhou, Y.F. & Shi, J.F. (2015).** Joint optimization of maintenance, buffer, and spare parts for a production system. *Applied Mathematical Modelling*, **39**(19): 6032-6042.

**Gershwin, S.B. (2018).** The future of manufacturing systems engineering. *International Journal of Production Research*, **56**(1-2): 224-237.

**Gershwin, S.B. & Schor, J.E. (2000).** Efficient algorithms for buffer space allocation. *Annals of Operations Research*, **93**: 117-144.

**Khan, B., Ahn, J.S. & Park, E.C. (2018).** An analysis framework for the performance of collocated heterogeneous wireless networks with negative acknowledgements. *Kuwait Journal of Science*, **45**(1): 70-78.

**Konishi, K. (2010).** A tuning strategy to avoid blocking and starving in a buffered production line. *European Journal of Operational Research*, **200**(2): 616-620.

**Kose, S.Y. & Kilincci, O. (2015).** Hybrid approach for buffer allocation in open serial production lines. *Computers & Operations Research*, **60**: 67-78.

**Matta A., M Pezzoni & Semeraro, Q. (2012).** A Kriging-based algorithm to optimize production systems approximated by analytical models. *Journal of Intelligent Manufacturing*, **23**: 587-597.

**Ng, A.H.C., Sabry, S. & Bernedixen, J. (2017).** Studying unbalanced workload and buffer allocation of production systems using multi-objective optimisation. *International Journal of Production Research*, **55**(24): 7435-7451.

**Papadopoulos, C.T., O’Kelly, M.E.J. & Tsadiras, A.K. (2013).** A DSS for the buffer allocation of production lines based on a comparative evaluation of a set of search algorithms. *International Journal of Production Research*, **51**(14): 4175-4199.

**Radhoui, M., Rezg, N. & Chelbi, A. (2009).** Integrated model of preventive maintenance, quality control and buffer sizing for unreliable and imperfect production systems. *International Journal of Production Research*, **47**(2): 389-402.

**Sabir, M.M. (2018).** Electrohydrodynamic flow solution in ion drag in a circular cylindrical conduit using hybrid

neural network and genetic algorithm. *Kuwait Journal of Science*, **40**(1): 93-107.

**Sabry, S., Tom, M. & Viatcheslav, D. (2017).** Asymmetrical buffer allocation in unpaced merging assembly lines. *Computers & Industrial Engineering*, **109**: 211-220.

**Sabuncuoglu, I., Erel, E. & Gocgun, Y. (2006).** Analysis of serial production lines: characterisation study and a new heuristic procedure for optimal buffer allocation. *International Journal of Production Research*, **44**(13): 2499-2523.

**Sana, S.S. (2012).** Preventive maintenance and optimal buffer inventory for products sold with warranty in an imperfect production system. *International Journal of Production Research*, **50**(23): 6764-6774.

**Shi, C. & Gershwin, S.B. (2016).** A segmentation approach for solving buffer allocation problems in large production systems. *International Journal of Production Research*, **54**(20): 6121-6141.

**Shu S.G. (1992).** Reliability analysis of computer integrated manufacturing system with buffers. *Acta Automatica Sinica*, **18**(1): 15-20.

**Staley, D.R. & Kim, D.S. (2012).** Experimental results for the allocation of buffers in closed serial production lines. *International Journal of Production Economics*, **137**(2): 284-291.

**Verma, M. & Kumar, M. (2013).** Performance analysis of 66/11 KV substation using Petri nets and vague lambda tau methodology. *Kuwait Journal of Science*, **45**(1): 20-28.

**Walid, A.K., Ozhand, G. & Fazle, B. (2011).** A nonlinear model for optimizing the performance of a multi-product production line. *International Transactions in Operational Research*, **18**(5): 561-577.

**Weiss S., Schwarz, J.A. & Stolletz, R. (2018).** The buffer allocation problem in production lines: Formulations, solution methods, and instances. *IIE Transactions* February, 1-30.

**Youssef, A.M.A. & ElMaraghy, H.A. (2008).** Performance analysis of manufacturing systems composed of modular machines using the universal generating function. *Journal of Manufacturing Systems*, **27**: 55-69.

**Submitted** : 03/05/2019

**Revised** : 02/02/2020

**Accepted** : 13/02/2020

**DOI** : 10.48129/kjs.v48i1.7789